Air filamentation characteristics of ring Airy femtosecond laser beam with different background energies

Hu Yuze, Nie Jinsong, Sun Ke, Wang Lei

(State Key Laboratory of Pulsed Power Laser Technology, Hefei 230037, China)

Abstract: Filamentation has stimulated growing research interest since the first observation of filament generated by an intense femtosecond laser pulse in air. Possible applications of filaments have also been proposed and demonstrated in laser induced electrical discharge particle acceleration, lidar remote sensing, THz radiation generation, and pulse compression. The characteristics of filamentation with a modulation of background energy distribution was presented by changing the confinement parameter of ring Airy beam numerically. The length of filaments longer than that of the Gaussian beam with faint background energy of the same peak power was achieved. By analyzing the spatial and temporal evolution progresses, it was found that the Airy beam airy-function-like energy distribution along radius of the background energy was the prerequisite to achieve peak intensity along the propagation direction. With comparison of spectra evolution consequences, it was found that the changing of the confinement parameter of Airy beam doesn´t have significant influence on the spectral broadening. But when changing the beam from ring Airy to Gaussian, the spectra is broadened dramatically.

Key words: femtosecond laser; Airy beam; Kerr-effect; self-focusing

CLC number: TN21 **Document code:** A **DOI:** 10.3788/IRLA201746.0806005

不同能量背景的环形艾里飞秒激光光束大气成丝特性

胡瑜泽,聂劲松,孙 可,王 磊

(脉冲功率激光技术国家重点实验室,安徽 合肥 230037)

摘 要: 自从第一次观察到飞秒激光大气成丝后,光丝备受科学家的关注。它的潜在应用价值主要包括电子加速、激光雷达远程遥感、太赫兹辐射和超短脉冲压缩。利用数值仿真的方法,通过改变艾里光束的衰减系数,研究了不同能量背景的环形艾里光束飞秒激光大气成丝特性,得到的光丝长度长于拥有相同峰值功率、弱能量背景高斯光束形成的光丝。通过分析飞秒激光光丝演化过程的时间和空间特性,发现了环形能量背景是环形艾里光束沿传播方向形成高能量密度光丝的前提条件。比较了环形艾里光束和高丝光束在成丝过程中的光谱展宽特性,发现不同衰减系数的环形艾里光束具有相似的光谱展宽特性,但要明显弱于高斯光束的光谱展宽。研究成果对与提升飞秒激光成丝效果具有参考意义。

关键词: 飞秒激光; 艾里光束; 克尔效应; 自聚焦

收稿日期:2016-12-05; **修订日期**:2017-01-03

作者简介:胡瑜泽(1993-),男,硕士生,主要从事飞秒激光方面的研究。Email:hyz_yj@sina.com

导师简介:聂劲松(1971-),男,教授,博士生导师,主要从事激光技术及其应用方面的研究。Email:njs7001@sina.com

0 Introduction

Filamentation induced by femtosecond laser pulses in gases has recently attracted considerable interest. The nonlinear effects experienced by filaments which are responsible for the self-guilded propagation are the optical Kerr effect and self-generated plasma defocusing [1]. Since some novel phenomena, such as plasma channel inside the filament and supercontinuum, the potential applications can be plentiful, like the analysis of air pollutants and atmospheric aerosol[2], laser induced lightning[3], rain making [4], coherent source in ultraviolet laser and X-ray[5], terahertz emission[6].

In order to prolong the length of filament, many approaches has been used in decades. The initial conditions of the beam have been changed by researchers using specific methods, such as changing the beam diameter [7], adding a temporal or spatial chirp to the beam [8-9], and forming a non-diffracting beam [10-12]. On the other hand, the background energy as a crucial role for long-distance propagation of filament has been proved both numerically and experimentally[13-14], showing that filaments are terminated due to the leakage of background energy caused by diffraction. The occurrences of these phenomena suggest that a longer filament can be achieved through a good design with the combination of initial beam profile and background energy distribution.

Airy beam, as one of the non-diffraction beams, has the property of self-healing[15], which can reserve more background energy than Gaussian beam. In this paper, we further study the elongation of filaments numerically by using a ring Airy beam to replace Gaussian beam and by changing the confinement parameter of Airy beam to modulate the background energy distribution. The characteristics, such as temporal and spatial intensity distribution profiles, plasma density and far-field spectrum of filaments will be demonstrated in details. Our results imply the length of filaments can be apparently prolonged through the modulation of the confinement parameter of Airy beam.

1 Numerical simulation model

In this work, the numerical simulation model can be divided into two parts of linear effects and nonlinear effects. Diffraction and group velocity dispersion(GVD) are taken into consideration as linear effects. The nonlinear responses of medium are composed of optical Kerr-effect, third harmonic generation, multiphoton ionization(MPI) and absorption of plasma. However, we ignore the Raman-effect, avalanche ionization and inverse bremsstrahlung absorption since 50 fs pulse width we use is not enough to produce these effects[16-18].

The nonlinear equation(2D+1 model) of filaments for the slowly varying amplitude $A(r,z,t)$ of the electric field[18] can be written as:

$$\frac{\partial A}{\partial z}=i\frac{1}{2k_0}\Delta_{\perp}A-i\frac{k^{*}}{2}\frac{\partial^2 A}{\partial t^2}+i\frac{k_0 n_2}{2}|A|^2A-ik_0\frac{n_e}{2n_c}A-\frac{\beta^{(K)}}{2}|A|^{2K-2}A \tag{1}$$

$$\frac{\partial n_e}{\partial t}=\frac{\beta^{(K)}}{K\hbar w_0}|A|^{2K}\left(1-\frac{n_t}{n_{at}}\right) \tag{2}$$

where the five terms of Eq.(1) represent diffraction, GVD, Kerr effect, the defocusing effect caused by plasma and absorption of multiphoton ionization, respectively. k_0, k', n_2, $\beta^{(K)}$, n_e, and n_{at} denote the wave number, coefficient of GVD, nonlinear index coefficient of Kerr-effect, multiphoton coefficient, the critical plasma density and neutral molecule density, respectively.

The model is solved via the Split-Step Fourier method, in which all the linear terms are calculated in the Fourier space over a half-step and the nonlinear terms are calculated in the physical space over a second half-step. For the Eq.(1), we adopt the Crank-Nicholson scheme.

When considering the third harmonic generation, the third harmonic envelope components of the

nonlinear polarization must be rewritten as:

$$P_{\omega 0}=\varepsilon_0\chi^{(3)}\frac{3}{4}[(|A_{\omega 0}|^2+2|A_{3\omega 0}|^2)A_{\omega 0}+A_{\omega 0}^{*2}A_{3\omega 0}] \quad (3)$$

$$P_{3\omega 0}=\varepsilon_0\chi^{(3)}\frac{3}{4}[(|A_{3\omega 0}|^2+2|A_{\omega 0}|^2)A_{3\omega 0}+A_{\omega 0}^{3}/3] \quad (4)$$

For both $P_{\omega 0}$ and $P_{3\omega 0}$, the first two items denote self-phase and cross-phase modulations and the last one represents third harmonic generation and back conversion. The relationship between and is:

$$P=\varepsilon_0\chi^{(3)}\frac{3}{4}|A|^2A \quad (5)$$

Without taking the atmosphere turbulence into consideration, the parameters we determine for this model are shown in Tab.1[18].

Tab.1 Parameters of the model in the air

Parameters	Values
k''	2.1×10^{-29} s^2/m
U_{air}	12.1 eV
n_{at}	1.5×10^{25} m^{-3}
$\beta^{(K=10)}$	1.27×10^{-126} cm^{17}/m^9
n_2	1×10^{-23} m^2/W
K	10

To solve the equations efficiently, the algorithms used are carried out in the transform regime. A split-step Fourier method is employed in the z-propagation direction, whereas the Hankel transform of zero-order and FFT are taken in the radial and temporal domain, respectively.

For the initial condition of the beam, the amplitude of the symmetrical ring Airy beam can be written as follows[10]:

$$A(r,z=0,t)=Ai(-|r|/r_0)\times\exp[-a|r|/r_0]\times\exp[-t^2/t_0^2] \quad (6)$$

where r is the radius, r_0 is a scale factor which determines the radius of the main lobe, and t_0 is the pulse width of temporal Gaussian beam. a is the so-called the confinement parameter of Airy beam which value is far less than 1 and the range of it is from 0.01 to 0.1 generally [19-20]. The energy distribution of side lobes can be changed dramatically with different values of a which will be changed in this paper as a modulation of background energy to elongate the length of filaments.

2 Simulation results

In this section, three ring Airy beam with a=0.1, 0.075, 0.05 and a Gaussian beam as a comparison are simulated under the same peak power. The characteristics like temporal and spatial intensity distributions, plasma density and far-field spectrum of filaments are compared in subsections.

Different profiles of beams can be easily attained through the phase mask and or spatial light phase modulator experimentally. In this case, as shown in Fig.1, we use four beams as initial conditions

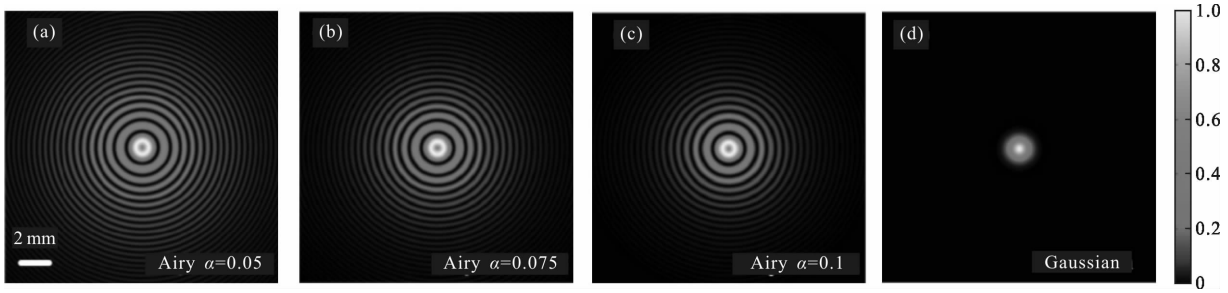

Fig.1 Intensity distributions of (a)-(c) ring Airy beams with peak power $P_m=5P_{cr}$ corresponding to the confinement parameters of 0.05, 0.075, 0.1 and (d) a standard Gaussian with the same peak power

representing different background energy distributions.

The peak power we used is five-fold to a critical value P_{cr}[17] given by:

$$P_{cr}=\frac{3.77\pi n_0}{2k_0^2n_2} \quad (7)$$

The transverse profiles of initial beams are

displayed in Fig.1 for the cases of (a)–(c) ring Airy beams with the scale factor of 0.5 mm, (d) Gaussian beam with the radius of 1 mm (1/e). The color distributions indicate that the energy of the side lobes of Airy beam can be modulated by different confinement parameters. Since the side lobes′ energy is far less than the main lobe, we consider the side lobes′ energy as background energy which is also called background energy reservoir.

2.1 Maximal intensity and plasma distribution along propagation direction

A quantity that is rather important to measure length of filaments is the maximal intensity against propagation distance where intensity clamping yields[21]. One could expect that if the background energy reservoir is not gathered tightly around the core of filaments and then, of course, diffraction would prevail. As a consequence, the outer part of background energy is escaped away, which is not in favor of elongating the filament. However, the Airy beam has a transverse acceleration lead side lobes to move to the main lobe. In this way, the energy leakage of outer part of background reservoir can be decreased.

Figure 2 shows that the maximal intensity as a function of propagation distance for the three ring Airy beams and a Gaussian beam. Fig.2 indicates that with the less confinement parameters, which means the more amounts of background energy it has, the longer length of filaments can be achieved whereas the Gaussian beam reaches the shortest since its faint energy reservoir.

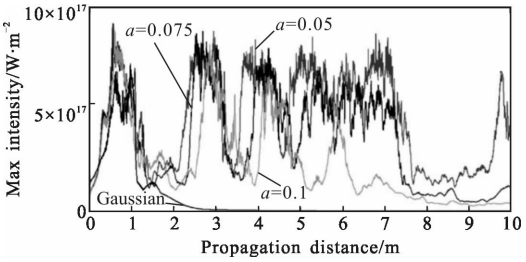

Fig.2 Maximal intensity versus propagation distance

Similar to the maximal intensity, the plasma generation is dramatically affected by the distribution of background energy. Figure 3(a) shows that the maximal plasma density as a function of propagation distance for the ring Airy beams and Gaussian beam as initial conditions shown in Fig.1. Figure 3(b) shows the total number of free electrons generated per unit length.

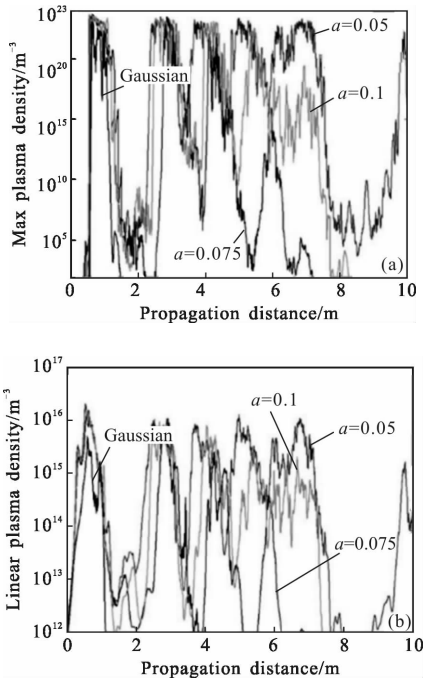

Fig.3 (a) Maximal plasma density and (b) Linear plasma density versus propagation distance

Based on Fig.2 and Fig.3, we can find that the first peak maximal intensity is obtained at the same position with approximate same value despite of what a background modulation it has when the pulse peak powers are equal. But if we take a look at the position afterward, the filament of Gaussian beam with a thin energy reservoir disappears at the first time and cannot get revival again. For the ring Airy beams, the background reservoir can be modulated by the confinement parameters. From the consequences, the repeating periods of filament have nothing with the change of confinement parameter while the number of recurring peaks have a tight correlation of the parameter. In other words, the lower value of confinement parameter meaning more energy saving in the side lobes, can obtain more number of times of peak intensity. In order to explain this phenomenon

completely, it is necessary to show more evolution details of these beams in the next section.

2.2 Spatial and temporal evolution

To show the process of how the propagation dynamics depend on initial conditions in details[22-24], the evolutional distributions of the filaments are depicted in this section. Thus, we calculate each filament in longitudinal plane to study the tracks of side lobes as an energy reservoir.

Figure 4 represents the energy evolution processes (a)-(c) ring Airy beams and (d) the Gaussian beam with parameters corresponding to Fig.1. The purple part of the profiles can be seen as the energy reservoir since the power is too low to cause intensity clamping. The distributions of filaments are the highlight part of the profiles.

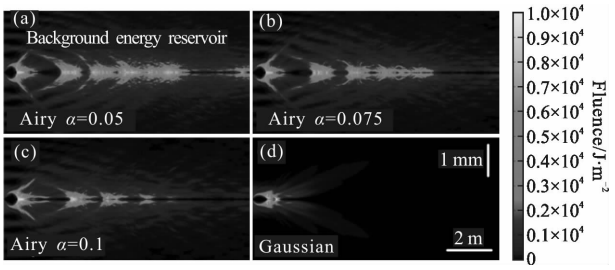

Fig.4 Calculated transverse fluence distributions along the propagation direction corresponding to (a)-(c) ring Airy beams with the confinement parameters of 0.05, 0.075, 0.1 and (d) a standard Gaussian respectively

As the Fig.4 shows, all these four beams start the filament at 0.5 m and reach the peak intensity firstly at 0.8 m. Compared with the Gaussian beam, it is clearly that all the Airy beams have the energy of radius-directional arrangement which self-focus gradually[25]. Then, if the first peak becomes weaker, the nearest wing of Airy beam will form the next peak intensity. This can be accounted that the Airy beam has the characteristic of self-healing as long as the main lobe of the beam becomes weaker, the wings′ energy will complement the loss of the crest automatically. So the self-healing of Airy beam can be used as a way to elongate the filament.

Another thing deserving our notice is that the energy reservoir of Airy beam is different from the Gaussian beam. If we look through the radial direction, the energy reservoir of Airy beam is under radius-directional arrangement whereas the Gaussian is continuous. Thus, the Kerr-effect of Gaussian beam to the background energy is more dramatic than Airy beam, which leads the Gaussian beam is more inclined to collapse. In this aspect, the modulation of background energy of filaments tough Airy beam has an inborn advantage than Gaussian beam.

Resulting the recurring periods of high peak intensity by the energy background of modulation can be studied through the envelop amplitude distributions as a function of time and radial distance (Fig.5) for several propagation distances before the peak intensity occurs.

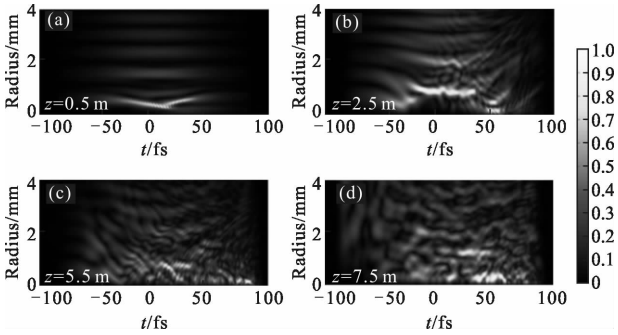

Fig.5 Filamentation dynamic of the envelope amplitude as a function of time at several distances corresponding to the confinement parameters 0.1. All are normalized according to the maximum amplitude

We use the ring beam of a=0.1 as an example to study what distribution of the energy could cause the repeat peak power of filaments. The distances of 0.5, 2.5, 5.5 m of Fig.5(a)-(c) are chosen because they are all before the peak intensity which means some of the characteristics could be found for why the repeating filaments are formed when compared with the envelope amplitude dynamic at the distance of 7.5 m(Fig.5(d)).

The pictures (a)-(c) of Fig.5 are before the peak intensity arrives whereas after (d) no peak intensity can obtain. The main distinction between these two cases is that the energy have a regular alignment along radial distance in the first case but the second

case tend to be disorder. When the Airy beam propagates longer distance the airy-function-like distribution will become more disorder. So, the characteristic of self-healing will be weaker, until the diffraction dominate the effects. It can be a strong evidence to prove that the modulation of background energy of Airy beams can be an efficient way to elongate filaments.

2.3 Spectral broadening

The spectral broadening of the femtosecond laser pulse is one of critical consequences of nonlinear interaction with mediums. Towards both the red side and the blue side, the spectra is mainly influenced by Self-Phase Modulation (SPM)[26-27].

In the femtosecond laser regime, the SPM can be divided into two parts: the front part of the pulse and the back part of the pulse which contributes principally to red shift and blue shift respectively.

$$\Delta\omega=-\frac{\omega_0 z}{c}n_2\frac{\partial I(\text{front part})}{\partial t}-\frac{\omega_0 z}{c}n_2\frac{\partial I(\text{steep back part})}{\partial t}+\frac{2\pi z e^2}{cm_e w_0}\frac{\partial N_e}{\partial t} \quad (8)$$

Here, n_2 is the Kerr nonlinear refractive index of air, I is the intensity.

On the right hand of Eq.(8), the first item causes red shift in the front part of the pulse and the left two items cause blue shift in the back part of the pulse. The last one is the plasma effect generated in the back part of the pulse.

Figure 6(a)-(c) displays the spectral broadening for three Airy pulses with different confinement parameters. From the consequence, the confinement parameter has little influence on the spectral broadening. But when the spatial shape function changed, the spectral broadening can be influenced dramatically.

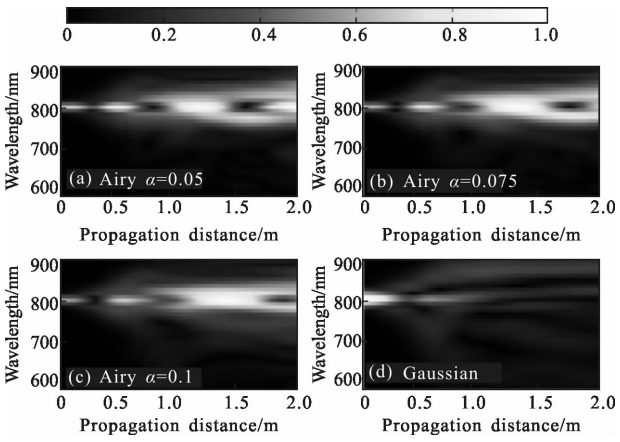

Fig.6 Pulses spectra as a function of propagation distance

3 Conclusions

We have investigated the filamentation by using a ring Airy beam as an initial condition. With the changing of the confinement parameter, the background energy of the beam can be modulated to a specific arrangement, which achieves the length of filaments almost ten times than the Gaussian beam of the same peak power with the faint background energy. It was demonstrated what tracks the modulated background energy undergo both spatially and temporally. Thus, for the Airy beam, a regulation was found that the airy-function-like modulation along radius of the background energy can be a prerequisite to achieve peak intensity again along the propagation direction. As for the spectral broadening, the changes of the confinement parameter of Airy beam didn′t show significant influences on it whereas the spectra were broadened more dramatically when changed it into a Gaussian beam.

References:

[1] Chin S L, Theberge F, Liu W. Filamentation nonlinear optics [J]. ***Appl Phys B***, 2007, 86(3): 477-483.

[2] Kasparian J, Rodriguez M, Méjean G, et al. White-light filaments for atmospheric analysis [J]. ***Science***, 2003, 301 (5629): 61-64.

[3] Guo K M, Lin J Q, Hao Z Q, et al. Triggering and guiding high-voltage discharge in air by single and multiple femtosecond filaments[J]. ***Opt Lett***, 2012, 37(2): 250-261.

[4] Rohwetter P, Kasparian J, Stelmaszczyk K, et al. Laser-induced water condensation in air[J]. ***Nat Photonics***, 2010, 4 (1): 451-456.

[5] Spielmann Ch, Burnett N H, Sartania S, et al. Generation of coherent X-rays in the water window using 5-femtosecond laser pulses[J]. ***Science***, 1997, 278(5338): 661-664.

[6] Bergé L, Skupin S, Köhler C, et al. 3D numerical simulations of THz generation by two color laser filaments [J]. ***Phys Rev Lett***, 2013, 110(1): 073901-073911.

[7] Luo Q, Hosseini S A, Liu W, et al. Effect of beam diameter on the propagation of intense femtosecond laser pulses [J]. ***Appl Phys B***, 2005, 80(1): 35-38.

[8] Park J, Lee J, Nam C H. Laser chirp effect on femtosecond laser filamentation generated for pulse compression [J]. ***Opt Express***, 2008, 16(7): 4465-4470.

[9] Xi Tingting, Zhao Zhijie, Hao Zuoqiang. Filamentation of femtosecond laser pulses with spatial chirp in air [J]. ***J Opt Soc Am B***, 2014,31(2): 321-324.

[10] Pavel Polynkin, Miroslav Kolesik, Jerome Moloney. Filamentation of femtosecond laser airy beams in water [J]. ***Phys Rev Lett***, 2009, 103(1): 123902-123912.

[11] Gao Hui, Sun Xiaodong, Zeng Bin, et al. Cylindrical symmetry breaking leads to multiple filamentation generation when focusing femtosecond lasers with axicons in methanol [J]. ***J Opt***, 2012, 14(6): 065203-065213.

[12] Polesana P, Franco M, Couairon A, et al. Filamentation in Kerr media from pulsed Bessel beams[J]. ***Phys Rev A***, 2008, 77(1): 043814-043824.

[13] Maik Scheller, Matthew S Mills, Mohammad-Ali Miri, et al. Externally refuelled optical filaments [J]. ***Nature Photonics***, 2014, 8(1): 297-301.

[14] Liu W, Gravel J F, Théberge F, et al. Background reservoir: its crucial role for long-distance propagation of femtosecond laser pulses in air[J]. ***A Phys B***, 2005, 80(7): 857-860.

[15] Pavel Polynkin, Miroslav Kolesik, Jerome V Moloney, et al. Curved plasma channel generation using ultraintense Airy beams[J]. ***Science***, 2009, 324(5924): 229-232.

[16] Bergé L, Skupin S, Lederer F. Multiple filamentation of Terawatt laser pulses in air [J]. ***Phys Rev Lett***, 2004, 92(1): 225002-225012.

[17] See Leang Chin. Femtosecond Lser Filamentation [M]. USA: Springer Science+Business Media, 2010.

[18] Sheng Zhengming. Advances in High Field Laser Physics[M]. Shanghai: Shanghai Jiaotong University Press, 2014.

[19] Shi Yaoyao, Wu Tong, Liu Youwen, et al. Control of self-bending airy beams [J]. ***Acta Photonica Sinica***, 2013, 42(12): 1401-1407.

[20] Panagiotopoulos P, Abdollahpour D, Lotti A, et al. Nonlinear propagation dynamics of finite-energy Airy beams[J]. ***Phy R A***, 2012, 1986: 1-15.

[21] Xu S, Bernhardt J, Sharifi M, et al. Intensity clamping during laser filamentation by TW level femtosecond laser in air and argon [J]. ***Laser Phys***, 2012, 22(1): 195-202.

[22] Liu Weiwei, Zhao Jiayu, Zhang Yizhu, et al. Research on superluminal propagation of terahertz wave during femtosecond laser filamentation [J]. ***Infrared and Laser Engineering***, 2016, 45(4): 0402001. (in Chinese)

[23] Yang Jing, Zhao Jiayu, Guo Lanjun, et al. Study of terahertz radiation from filamentation induced by ultrafast[J]. ***Infrared and Laser Engineering***, 2015, 44(3): 996-1007. (in Chinese)

[24] Bai Ya, Xu Rongjie, Song Liwei, et al. Enhanced far field terahertz in forward direction due to relative phase flatten of two-color field [J]. ***Infrared and Laser Engineering***, 2014, 43(8): 2656-2661. (in Chinese)

[25] Wu Dongjiang, Zhou Siyu, Yao Longyuan, et al. Simulation of micro-groove cross-section in femtosecond laser ablation of quartz glass [J]. ***Infrared and Laser Engineering***, 2015, 44(8): 2243-2249. (in Chinese)

[26] Ren Yu, Li Fujin, Dong Xu, et al. Research of guiding energy with plasma channel induced by femtosecond laser in air[J]. ***Chinese Optics***, 2012, 5(2): 133-142. (in Chinese)

[27] Wang Ming, Wang Tingfeng, Shao Junfeng. Analysis of femtosecond laser induced damage to array CCD camera[J]. ***Chinese Optics***, 2013, 6(1): 96-102. (in Chinese)